On the optical and morphological properties of microstructured Black Silicon obtained by cryogenic-enhanced plasma reactive ion etching

K. N. Nguyen, Philippe Basset, F. Marty, Yamin Leprince-Wang, Tarik Bourouina

▶ **To cite this version:**

K. N. Nguyen, Philippe Basset, F. Marty, Yamin Leprince-Wang, Tarik Bourouina. On the optical and morphological properties of microstructured Black Silicon obtained by cryogenic-enhanced plasma reactive ion etching. Journal of Applied Physics, 2013, 113 (19), 10.1063/1.4805024 . hal-01721058

HAL Id: hal-01721058
https://hal.science/hal-01721058v1

Submitted on 25 May 2022

HAL is a multi-disciplinary open access archive for the deposit and dissemination of scientific research documents, whether they are published or not. The documents may come from teaching and research institutions in France or abroad, or from public or private research centers.

L'archive ouverte pluridisciplinaire **HAL**, est destinée au dépôt et à la diffusion de documents scientifiques de niveau recherche, publiés ou non, émanant des établissements d'enseignement et de recherche français ou étrangers, des laboratoires publics ou privés.

Journal of Applied Physics

On the optical and morphological properties of microstructured Black Silicon obtained by cryogenic-enhanced plasma reactive ion etching

Cite as: J. Appl. Phys. **113**, 194903 (2013); https://doi.org/10.1063/1.4805024
Submitted: 13 February 2013 • Accepted: 29 April 2013 • Published Online: 16 May 2013

K. N. Nguyen, P. Basset, F. Marty, et al.


View Online

Export Citation

CrossMark

ARTICLES YOU MAY BE INTERESTED IN

The structural and optical properties of black silicon by inductively coupled plasma reactive ion etching
Journal of Applied Physics **116**, 173503 (2014); https://doi.org/10.1063/1.4900996

Nanostructured black silicon and the optical reflectance of graded-density surfaces
Applied Physics Letters **94**, 231121 (2009); https://doi.org/10.1063/1.3152244

A theoretical study on the optical properties of black silicon
AIP Advances **8**, 035010 (2018); https://doi.org/10.1063/1.5018642

Lock-in Amplifiers up to 600 MHz
Zurich Instruments
Watch


AIP Publishing

© 2013 AIP Publishing LLC.

On the optical and morphological properties of microstructured Black Silicon obtained by cryogenic-enhanced plasma reactive ion etching

K. N. Nguyen,[1] P. Basset,[1] F. Marty,[1] Y. Leprince-Wang,[2,a)] and T. Bourouina[1]
[1]*Université Paris-Est, ESYCOM (EA 2552), UPEMLV, ESIEE-Paris, CNAM F-93162 Noisy-le-Grand, France*
[2]*Université Paris-Est, LPMDI (EA 7264), UPEMLV, F-774554 Marne-la-Vallée, France*

(Received 13 February 2013; accepted 29 April 2013; published online 16 May 2013)

Motivated by the need for obtaining low reflectivity silicon surfaces, we report on (sub-) micro-texturing of silicon using a high throughput fabrication process involving SF_6/O_2 reactive ion etching at cryogenic temperatures, leading to Black Silicon (BS). The corresponding high aspect ratio conical spikes of the microstructured surface give rise to multiple reflections and hence, enhanced absorption under electromagnetic radiation. Aiming a better understanding of this mechanism, we performed a systematic study by varying several plasma process parameters: O_2/SF_6 gas flow rate ratio, silicon temperature, bias voltage, and etching time. We determined the process window which leads to BS formation and we studied the influence of the process parameters on the surface morphology of the obtained BS samples, through analysis of scanning electron microscopy images. The measured optical reflectance of BS is in the order of 1% in the visible and near infrared ranges (400–950 nm). We noticed that the lowest reflectance is obtained close to the threshold parameters of BS formation. Absorptance spectral response of BS is measured from 1.3 to 17 μm, and we observed a great enhancement of absorptance up to about 75% compared to flat silicon. We also obtained through these experiments, a clear evidence of a correlation between the excellent optical properties and the aspect ratio of the BS conical microstructures in the measured wavelength ranges. © *2013 AIP Publishing LLC*. [http://dx.doi.org/10.1063/1.4805024]

I. INTRODUCTION

Silicon is a widely used semiconductor for the fabrication of optoelectronic devices thanks to the developed processing facilities of silicon microtechnology. However, flat silicon surfaces have high natural reflectance of around 30%–40%, also strongly depending on the wavelength range. For this reason, different solutions to reduce the reflection losses caused by the light specular reflection on the polished silicon were considered. Usually, an anti-reflection transparent layer such as ZnO, TiO_x, SiO_x, or SiN_x with quarter wavelength thicknesses is used.[1–3] However, the reduction of the reflection of these layers is effective only over a limited spectral range. Another way of reducing reflection is surface texturing, which is one of the most effective techniques to reduce silicon reflectance surface over wide band. It is a light trapping scheme within the silicon structure, which eventually reduces the effective reflectance, due to multiple reflections of the incident light (Fig. 1) and, therefore, to a more efficient light absorption in the silicon volume. The (sub-)micro textured silicon surface can be formed in various shapes (spikes, "penguin-like" structures, columns, and pyramids) and results in a black surface to the naked eye, hence the name "black silicon" (BS). BS is now recognized as an antireflective layer both in visible and infrared ranges;[4–6] hence, it attracted attention for numerous applications, including solar cells,[7–10] improved IR photodetector,[11,12] and photothermal conversion.[13] On the other hand, other remarkable surface properties of BS led to various applications such as biomedical devices,[14] thermoelectric harvesters,[15] superhydrophobic coatings,[16,17] and silicon-based luminescence devices.[18,19]

Several approaches have been developed to minimize the reflection losses of silicon by texturing the surface. The techniques of silicon texturing by reactive ion etching (RIE)[20–22] and inductively coupled plasma-reactive ion etching (ICP-RIE), also known as deep reactive ion etching (DRIE),[23–25] have been reported. Black silicon can be formed with high throughput and over a wide area without using a lithography mask. It is achieved in a single step within a few minutes by DRIE using an inductively coupled plasma of sulphur hexafluoride (SF_6) and oxygen (O_2) at cryogenic temperatures. DRIE allows anisotropic etching of silicon by taking advantage of passivation mechanism in the sidewalls. This method is fairly simple, rapid, and controllable.[26,27] Besides, silicon wet etching, not considered in this paper, can also lead to inverted pyramids or to concave pits.[28–30] The structuring of silicon using maskless femtosecond laser in SF_6 resulting in the form of micro and sub-micro silicon cones is also well developed.[31–33] This is an important process for the black silicon formation but the equipment investment of this technique is relatively heavy and the process usually takes a long duration due to the need for laser scanning over the whole substrate surface.

In this paper, we present a systematic study of the black silicon formation by varying the DRIE process parameters under cryogenic temperatures. Different shapes and sizes

a)Author to whom correspondence should be addressed. Electronic mail: yamin.leprince@univ-paris-est.fr.

 © 2013 AIP Publishing LLC

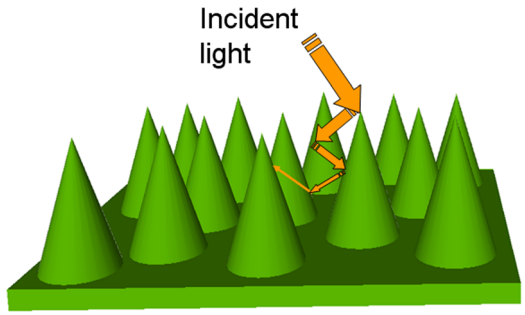

FIG. 1. Schematic representation of black silicon by conical microstructures illustrating the multiple reflection of incident light.

(micro and/or sub-micrometer) of BS structures with a high aspect ratio are obtained within specific conditions of an experimental process window. The morphological and structural properties of BS are characterized using scanning electron microscopy (SEM). Reflectance and absorptance measurements of these textures are achieved in both visible and infrared spectral ranges. Among our objectives through this study is to obtain a variety of high aspect ratio BS structures and then relate their characteristic dimensions to the corresponding reflectance and absorptance in the visible and infrared ranges. To the best of our knowledge, no such investigation has been reported to date.

II. EXPERIMENTAL DETAILS

Silicon is etched by DRIE process at cryogenic temperatures. BS with random microstructures is obtained in a plasma compound of SF_6 and O_2 under controlled process conditions. It is important at this stage to briefly recall the mechanism of this process; SF_6 gases produce fluorinated radicals F^* for chemical etching of silicon leading to volatile SiF_4, which can be described as

$$Si + 4\,F^* \rightarrow SiF_4. \quad (1)$$

Simultaneously, the fluorinated radicals react with the silicon by forming SiF_x sites on its surface, which then react with the oxygen radicals O* for the formation of sidewall passivation layers SiO_yF_x. This passivation layer plays a very important role in the BS formation.

$$Si + x\,F^* \rightarrow SiF_x, \quad (2)$$

$$SiF_x + y\,O^* \rightarrow SiO_yF_x. \quad (3)$$

There are several parameters that influence the process, such as electrical power, pressure, SF_6 and O_2 flow rates, bias voltage, temperature, and etching time. The role of each parameter is known in the case of classical RIE. But in the particular case of the BS formation, the main influential parameters are the O_2 flow rate and the etching temperature. Indeed, the presence of oxygen determines the formation of the passivation layer SiO_yF_x, and this layer is essential for the BS formation.[34,35] In addition, this passivation layer is formed only at cryogenic temperatures and it is volatile at room temperature. That is why it is essential to operate at cryogenic temperatures to obtain black silicon.

TABLE I. The variable parameters of cryogenic DRIE process. The values shown in bold are fixed while making changes to any settings.

Ratio O_2/SF_6	0.02	**0.05**	0.10	0.15	0.25	
Temperature (°C)	−80	−90	−100	−110	**−120**	−130
Bias voltage (V)	0	**−10**	−20	−30	−40	
Etching time (min)	2	5	**10**	20	30	

Fabrication of the BS samples under consideration in this study was carried out using an industrial reactor *Alcatel 601E*. A series of BS samples were prepared to study the influence of different process parameters. The fixed parameters for all samples are ICP power of 1000 W, gas pressure of 1.5 Pa, and SF_6 gas flow rate of 200 sccm. The variable parameters are the gas flow rate ratio O_2/SF_6, the temperature of the silicon wafer, the bias voltage, and the etching time. These parameters are summarized in Table I. When a given process parameter is varied, the bold characters indicate the fixed values of the other parameters. The samples were produced on single side polished (100)-oriented single crystalline silicon wafers of 4 in.-diameter, with a resistivity

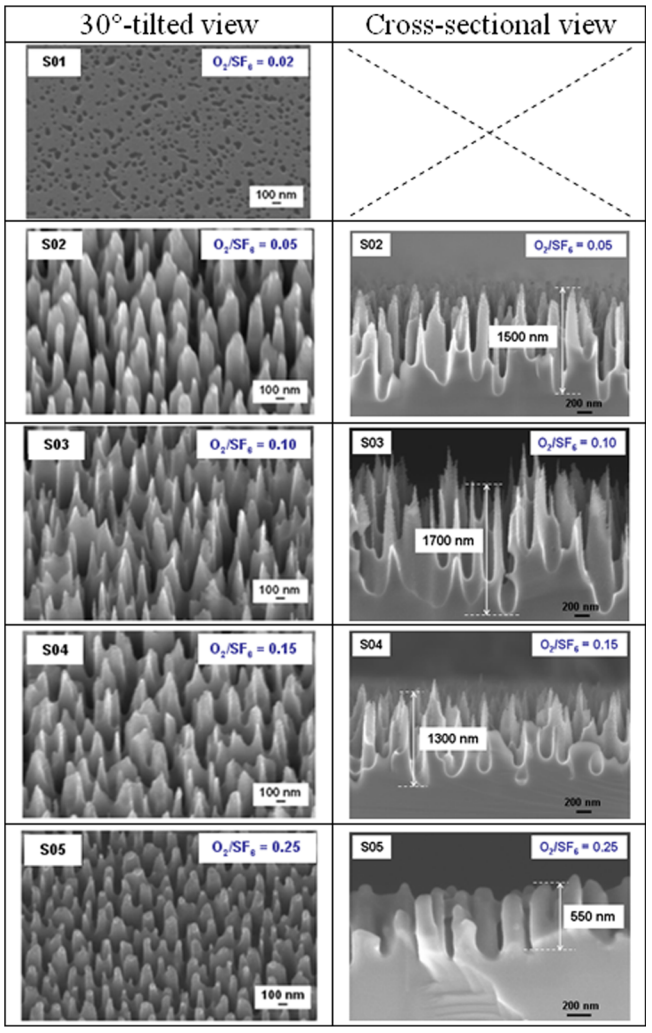

FIG. 2. SEM images with 30°-tilted and cross-sectional view of samples with different ratios O_2/SF_6: 1000 W, 1.5 Pa, 200 sccm SF_6, −120 °C, −10 V, 10 min.

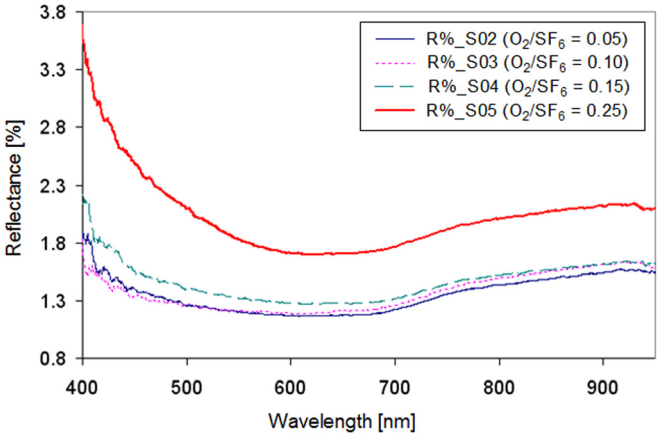

FIG. 3. Measured reflectance spectra in the visible and near infrared ranges of BS samples obtained at different O_2/SF_6 ratios.

of 1-20 Ω·cm and thickness of 525 μm, on which several square samples of 1 cm^2 have been prepared.

The morphological micro/nanostructures of the BS have been characterized using scanning electron microscope (FEG-SEM, NEON 40 - Carl Zeiss). Analyzing the top-view SEM images by Fourier Transform (FT) leads to the characteristic size of the BS structures, also referred as *pseudo-periodicity*. We mainly base on morphological observations through SEM images to perform a preliminary study of the influence of etching process parameters. The corresponding optical reflectance of the resulting BS surfaces is also recorded to study the influence of these process parameters.

We investigated the BS formation process systematically by varying the different parameters of DRIE process summarized in Table I, leading to 16 different samples where BS was effectively formed among the 21 case studies.

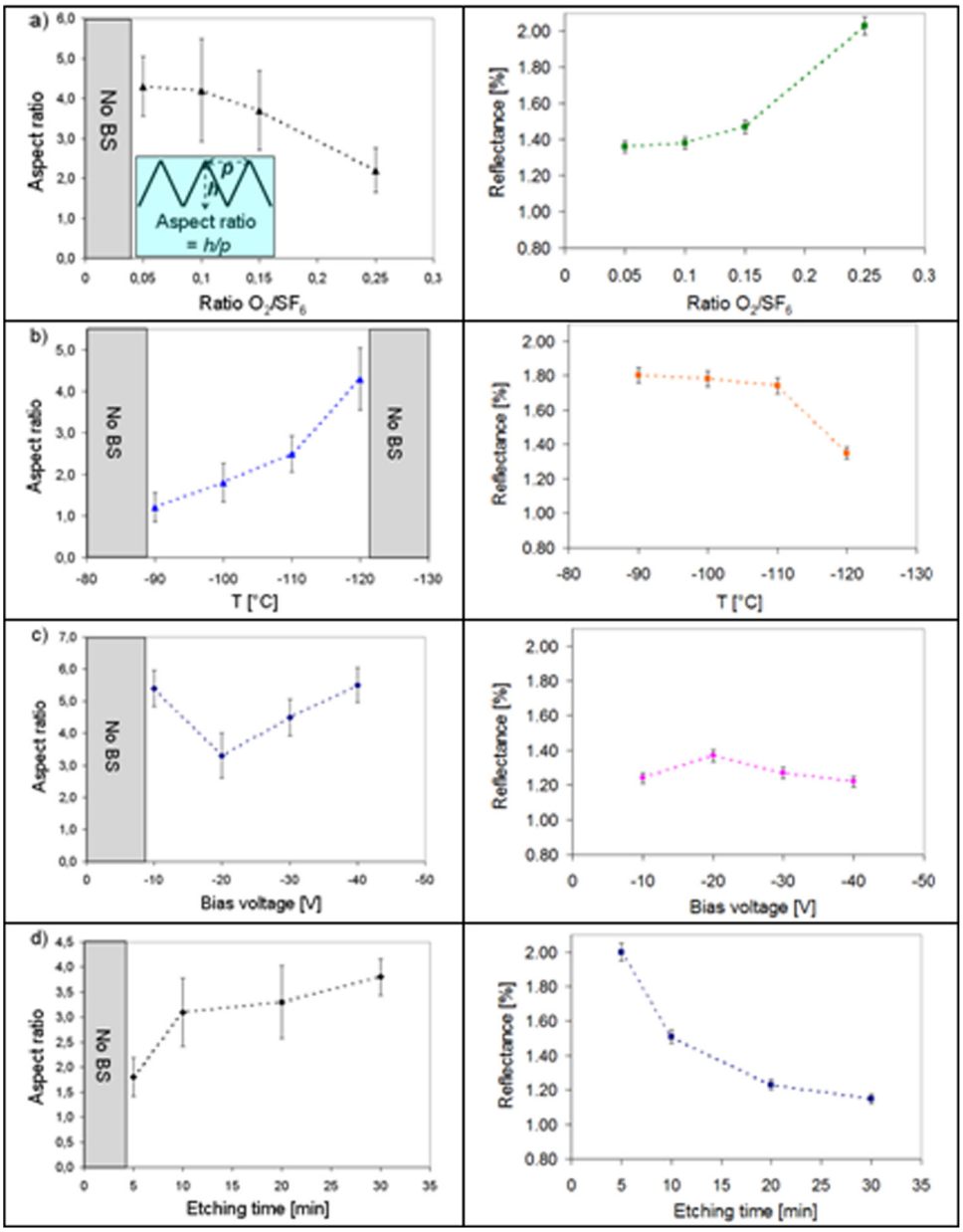

FIG. 4. Aspect ratio and average reflectance of BS samples (a) vs. O_2/SF_6 ratio. Inset: sketch of aspect ratio of BS structure. (b) vs. temperature, (c) vs. bias voltage, and (d) vs. etching time.

III. CHARACTERIZATION RESULTS AND DISCUSSION

A. Influence of the O_2/SF_6 ratio of flow rates

The fabrication results are illustrated in detail when varying the O_2/SF_6 ratio of flow rates from 0.02 to 0.25. Fig. 2 shows SEM images with 30°-tilted view and in cross-section view of the corresponding samples. Recall that the oxygen content in SF_6/O_2 plasma plays a very important role in the formation of the SiO_yF_x passivation layer. This is a crucial factor for the anisotropy of cryogenic DRIE, from which the interest to carry out this study initially stemmed. This suggests that the O_2/SF_6 ratio of flow rates might have some influence on the formation of BS; at a constant temperature and at fixed ion energy, the BS formation is indeed expected to depend only on the oxygen content. We experimentally noticed that the BS is formed only starting from the O_2/SF_6 ratio of 0.05. This also means that for insufficient oxygen content ($O_2/SF_6 = 0.02$, for example), there is no BS formation. Instead, we observed some porosity of the silicon surface. We understand that this is due to the insufficient thickness of the passivation layer SiO_yF_x, which is not resistant enough to the ionic bombardment for reaching the threshold limit.

Furthermore, we obtained different types of BS structures when the O_2/SF_6 ratio is varied from 0.05 to 0.15 (S02, S03, and S04) with isolated and homogeneous points, whose heights are in micrometer range (1300 to 1700 nm), and of "penguin-like" structures (S05) with height of submicrometer size (550 nm) when the O_2/SF_6 ratio reached 0.25. We would like to note that the height (h) of the BS samples was investigated directly from SEM images and represents the maximum values of the relief (Fig. 2).

The pseudo-periodicity (p) of BS samples was obtained by the FT analysis of the top-view SEM images.[16,36] The aspect ratio is then calculated as the ratio between the height (h) and the pseudo-periodicity (p).

Reflectance measurements have been performed in the visible and near infrared ranges (400–950 nm), using the spectrometer Maya 2000 Pro from Ocean Optics equipped with a fiber-coupled halogen light source and an integrating sphere. Reflectivity standards have been used for calibration. Fig. 3 plots the measured reflectance of the BS samples shown in Fig. 2 when the ratio O_2/SF_6 varied. The average reflectance $R\%$ in the spectral range (400 nm–950 nm) of BS samples is calculated and will be then taken as a reference in the Secs. III B–III F to compare the different samples.

Fig. 4(a) plots the aspect ratio and the average reflectance of BS samples at different O_2/SF_6 ratios. We noted here that for estimating uncertainty of the aspect ratio (h/p) of BS, we have calculated the errors on h and p for each BS sample, while the estimated error of 2% for the average reflectance R was evaluated from the measured values of the BS. It is observed that the reflectance of BS samples increases with the O_2/SF_6 ratio. First, when the ratio O_2/SF_6 varies in the range of [0.05, 0.10, 0.15], we observe that the average reflectance $R\%$ changes slightly [1.36%, 1.38%, 1.47%]. However, when this ratio increases from 0.05 to 0.25, we observe a more important increase in the reflectance from 1.36% to 2.03%, which is due to the decrease of the structure's height (the aspect ratio of the BS decreases by a factor of two in this case). We noticed that the aspect ratio of the black silicon decreases by a factor of two when the O_2/SF_6 ratio is varied from 0.05 to 0.25. On one hand, the largest aspect ratio occurs in the case of the microstructure of peaks corresponding to the threshold of BS formation, at the ratio O_2/SF_6 of 0.05. On the other hand, the minimum of the average reflectance is also obtained at this ratio. Hence, the ratio O_2/SF_6 of 0.05 was chosen as the fixed parameter in the following BS fabrication experiments.

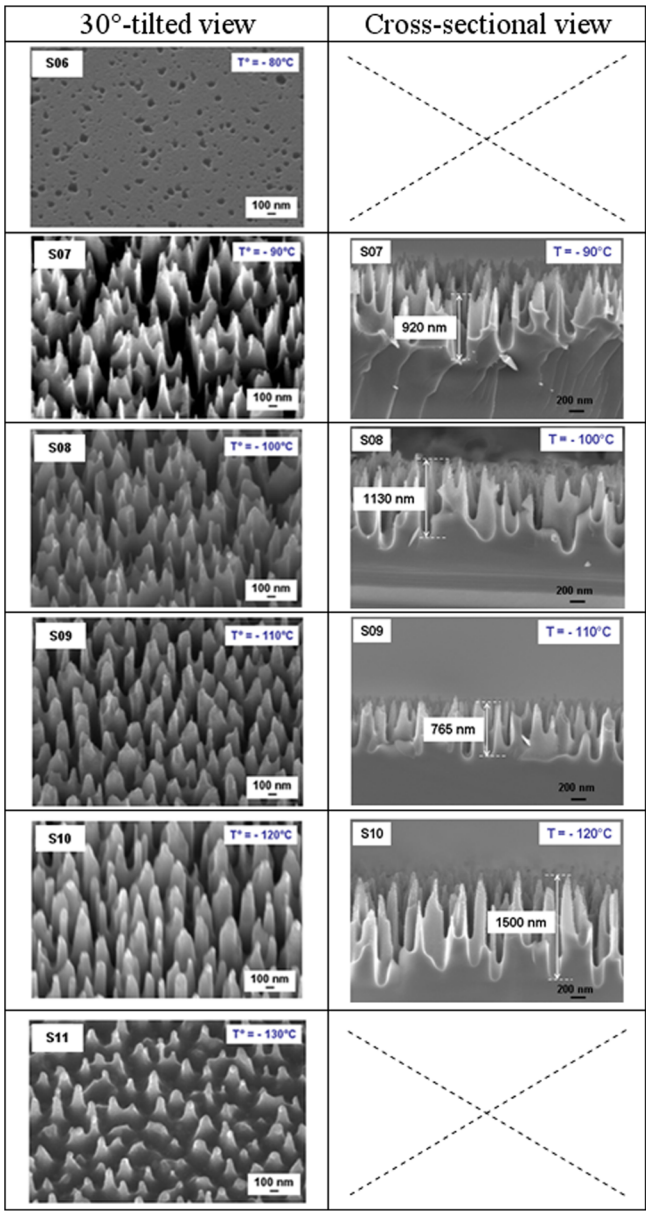

FIG. 5. SEM images with 30°-tilted and cross-sectional view of samples with different temperatures ranging from −80 °C to −130 °C (fixed parameters are 1000 W, 1.5 Pa, 200 sccm SF_6, 0.05 O_2/SF_6, −10 V, 10 min).

B. Influence of substrate temperature

We studied the effect of temperature on the BS fabrication by varying its value from −80 °C to −130 °C with the O_2/SF_6 ratio fixed at 0.05. First, we noted that under our conditions (1000 W, 1.5 Pa, 200 sccm SF_6, $O_2/SF_6 = 0.05$,

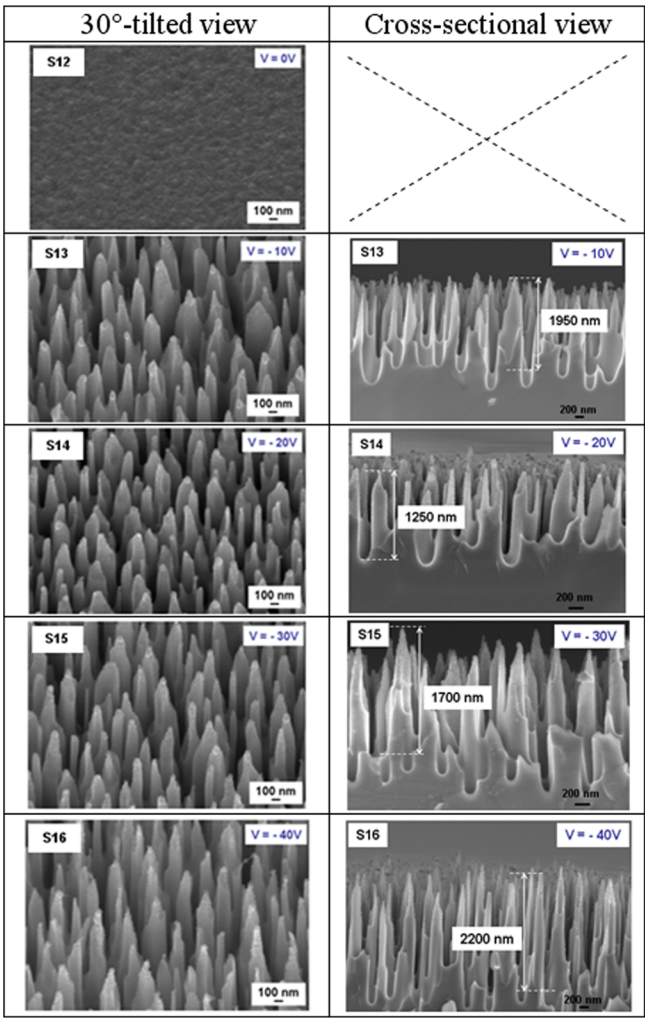

FIG. 6. SEM images with 30°-tilted and cross-sectional view of samples with different bias voltages (fixed parameters: 1000 W, 1.5 Pa, 200 sccm SF_6, 0.05 O_2/SF_6, −120 °C, 10 min).

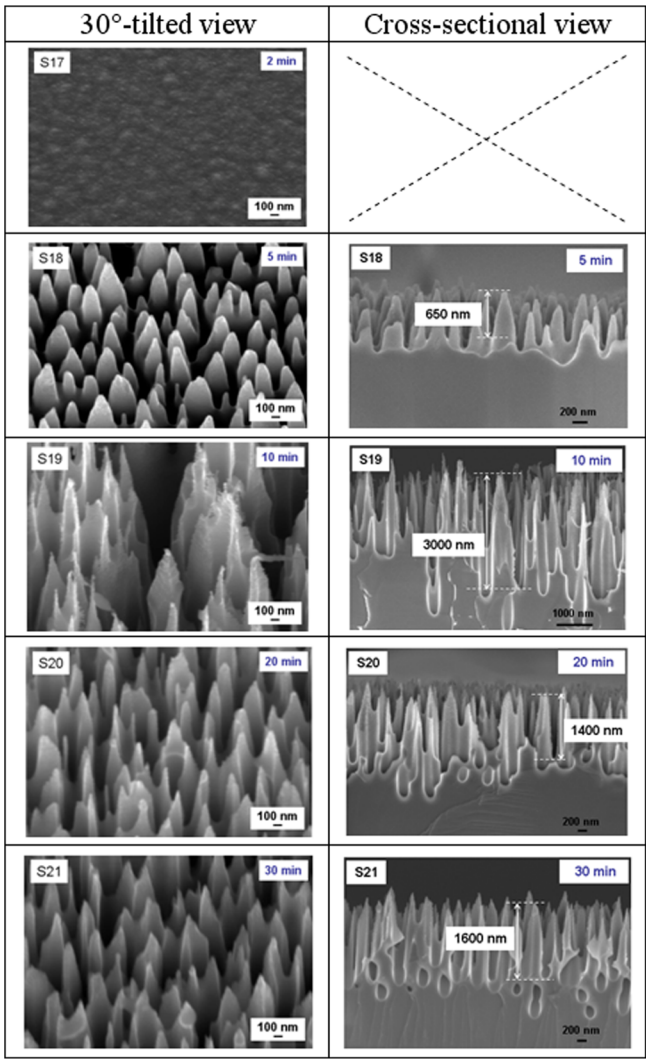

FIG. 7. SEM images with 30°-tilted and cross-sectional view of samples with different etching times from 2 to 30 min (fixed parameters 1000 W, 1.5 Pa, 200 sccm SF_6, 0.05 O_2/SF_6, −120 °C, −10 V).

−10 V, 10 min), the BS is formed only in a temperature range between −90 and −120 °C. Fig. 5 summarizes the SEM observations of these samples showing different types of BS structure.

Sample S06 obtained at the temperature of −80 °C has a roughened surface but not black after etching. Whereas sample S11 formed at the temperature of −130 °C has a "penguin-like" structure and revealed a dark-gray tone. Therefore, we can assume that at these temperatures, with a selected oxygen content, the passivation layer SiO_xF_y is either not resistant enough (S06) or are too resistant (S11) to the ion bombardment.

From the SEM images with 30°-tilted view of BS samples, we can observe a BS structure change from the type of "curvilinear way" as witnessed in sample S07, with an alternation of the black colour "drains" and various zones of the fine points, to the type of the homogeneous and dense points, as seen in sample S10. The SEM images in cross-sectional view of BS samples confirm that the structure becomes more uniform and dense from −110 °C onwards. When the temperature decreases to −120 °C, an anisotropic structure of isolated and homogeneous spikes is obtained, owing to increased resistance of the passivation layer. The spikes height also becomes more important at this temperature.

Fig. 4(b) represents the aspect ratio and the average reflectance of BS samples following the variation of the temperature. It is observed that the aspect ratio of BS structure rises when the temperature decreases and attains the

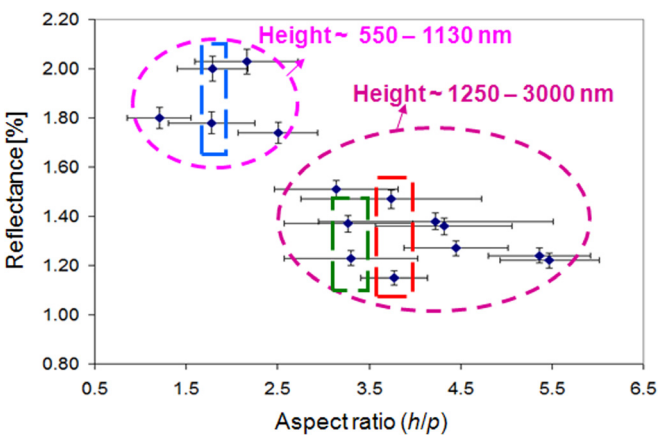

FIG. 8. Average reflectance of BS structures.

TABLE II. Three groups of BS samples with the same aspect ratio but different reflectances.

Sample	Aspect ratio	Height [nm]	Average R [%]
S18	1.8	650	2.00
S08	1.8	1130	1.78
S14	3.3	1250	1.37
S20	3.3	1400	1.23
S04	3.7	1300	1.47
S21	3.8	1600	1.15

maximum value at the threshold (−120 °C) of the BS formation. Indeed, we find an increase by a factor of four while comparing S07 and S10, which correspond to the temperatures of −90 °C and −120 °C, respectively. The average reflectance of the threshold BS structure (S10) also corresponds to the minimum value. In the following processes, the temperature is hence fixed at −120 °C.

C. Influence of the bias voltage

The influence of the bias voltage on the formation of black silicon will be studied by varying it from 0 to −40 V under the following fixed conditions: 1000 W, 1.5 Pa, 200 sccm SF_6, 0.05 O_2/SF_6, −120 °C, 10 min.

In cryogenic etching, the bias voltage controls the energy and direction of the ions which arrive at the surface of silicon. Under our conditions, the BS is formed starting from the bias voltage of −10 V. In the case of etching without potential bias, the BS did not form (S12), on which a roughened surface was produced uniformly. Fig. 6 shows the morphological evolution of black silicon structures when the bias voltage varied from −10 to −40 V. The SEM images obtained with 30°-tilted view show that all the four BS samples (S13, S14, S15, and S16) present the same type of microstructures owning isolated points. The aspect ratio and the average reflectance of these structures vary slightly between two values of the bias voltage of −10 V and −40 V (see Fig. 4(c)). The variation of the bias voltage in this case obviously does not have much influence on the characteristic dimensions and the reflectance of BS. Sample S14, which was obtained at a bias voltage of −20 V, reveals the highest reflectance and in the same time it exhibits the smallest aspect ratio.

D. Influence of etching time

To evaluate the effect of the etching time on the BS formation, we performed a study with the following fixed parameters: 1000 W, 1.5 Pa, 200 sccm SF_6, 0.05 O_2/SF_6, −120 °C, −10 V, whereas the duration of etching time varied from 2 to 30 min.

As shown in the SEM images with 30°-tilted view of these samples (see Fig. 7), a complex evolution of the BS structures is noted when the duration of etching changes. The sample of black silicon S18 obtained after 5 min of etching presents a sub-micron "penguin-like" structure. After 10 min, a structure (S19) of micrometric size is obtained. The cross-sectional observation of this sample shows that there are groups of submicron-size peaks covering the cones in micrometer size. An increase of the aspect ratio (from 1.8 to 3.1) is noticed by comparing the two samples S18 (5 min) and S19 (10 min). When the etching time increases to 20 min (S20) and 30 min (S21), we observe the same type of structures with fairly homogeneous peaks of micro and submicrometric size. However, we obtain a structure with sharper and more homogeneous peaks in the case of S21 and the aspect ratio increases to the value of 3.8.

Fig. 4(d) shows a plot of the aspect ratio of BS structures and their average reflectance in the spectral range of 400–950 nm vs etching time. We can conclude that in the case of the BS formation, the aspect ratio of the BS structure increases with the etching duration. The BS structure with largest aspect ratio represents the minimum reflectance in the visible and near infrared ranges.

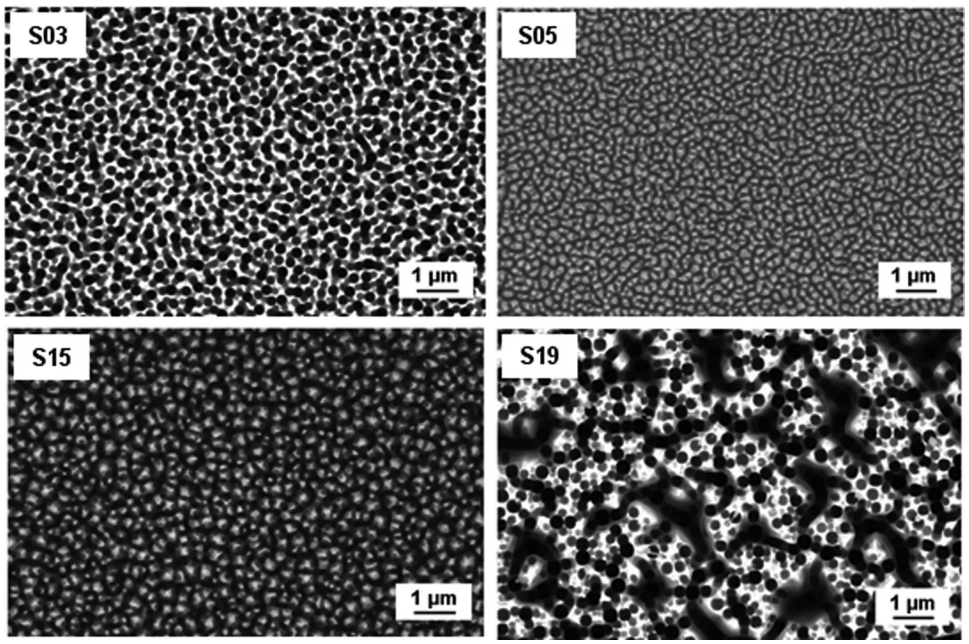

FIG. 9. Top-view SEM images of BS samples S03, S05, S15, and S19.

TABLE III. Characteristic dimensions of BS samples S03, S05, S15, and S19.

Sample	Structure	Period (nm)	Height (nm)	Aspect ratio	Average reflectance (%)
S03	Structure of isolated quasi-circular holes and fine peaks	402	1700	4.2	1.38
S05	"Penguin-like" structure of small period and submicron size	255	550	2.2	2.03
S15	Structure with isolated points of uniform size	382	1700	4.5	1.27
S19	Structure with large period and micron size	955	3000	3.1	1.51

E. Correlation between average reflectance, aspect ratio, and height of the BS structures

In Secs. III A–III D, the measurements of reflectance in the visible and near infrared for all our BS samples were investigated. It is also to be noted that our best BS samples behave as anti-reflected surfaces with an average reflectance of about 1% in the visible and near infrared ranges. Fig. 8 represents the average reflectances of all BS samples obtained in our work, and we found clear evidence that the reflectance decreases when the aspect ratio increases. Two groups of samples with different heights can be distinguished: one group where the height varies from 550 to 1130 nm and a second group with greater heights, ranging from 1250 to 3000 nm. We also note three sub-groups of BS samples whose aspect ratio is nearly identical in each group but having different reflectances. These sub-groups are (S18, S08), (S14, S20), (S04, S21), and are represented also in Table II. It is found that the reflectance of BS within each sub-group is inversely proportional to the height of the structure: the greater the height, the smaller the average reflectance. These observations let us assess the correlations between morphological and optical properties of our BS samples. Those results are also in agreement with our simulation results of the optical reflectance in the visible and infrared ranges.[37]

F. Absorptance of black silicon in infrared range

The absorption of black silicon structures in infrared spectral range has been investigated in this section. We have chosen four typical BS samples (S03, S05, S15, and S19), which represent the four morphological varieties of the obtained BS samples. Indeed, the different geometries of the samples can be more clearly seen from the top-view SEM images (Fig. 9). The structure description and the characteristic dimensions of these samples are summarized in Table III.

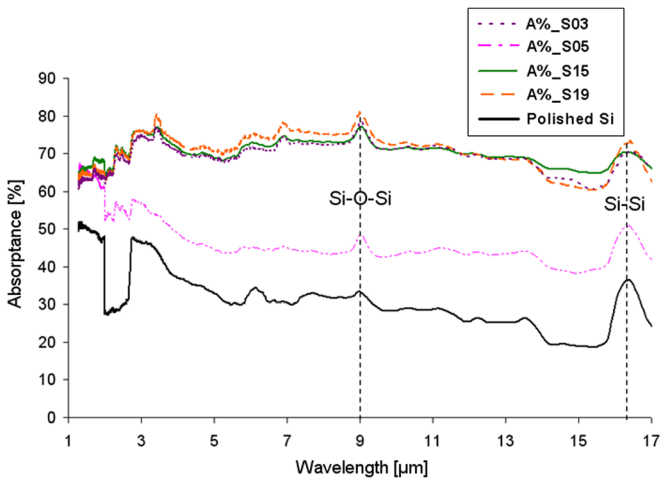

FIG. 10. Absorptance spectra in infrared ranges (1.3 μm–17 μm) of BS structures compared with polished flat silicon.

The reflectance (R) of BS samples and polished silicon were measured using Vertex 70 FT-IR spectrometer equipped with an integrating sphere. The measurements of transmittance (T) in infrared spectral range were performed by using an FT-IR spectrometer (Perkin Elmer Paragon 1000). The absorptance (A) of the samples was obtained via the relation $A = 1 - R - T$.

The absorptance spectra of BS samples and the unstructured silicon in the wavelength range from 1.3 to 17 μm are shown in the Fig. 10. It should be noted that the absorption peaks observed at $\sim$9 μm are assigned to the stretching vibration of Si-O-Si bond, while the other peak observed at $\sim$16.2 μm is due to the stretching vibration of Si-Si bond of bulk silicon.[38,39]

We noted an enhancement of BS absorptance while compared to the flat silicon that presents an infrared absorption of about 30%. The infrared absorption is strongly related to the aspect ratio of the BS. The higher the aspect ratio is, the greater the absorptance. In our study, we can distinguish two groups of black silicon samples: one (S05) with low aspect ratio ($\sim$2) showing an absorptance in the order of 50%; while the other one (S03, S15, and S19) with higher aspect ratio ($\sim$3–4) presents an absorptance of about 75%. We also noted the specific absorption peaks of our BS samples comparing to the polished silicon, such as peaks at 3.5 μm and 6.7 μm and we observed that these peaks become more significant in the case of higher aspect ratio group. Although the lower aspect ratio of S19 compared to S03 and S15, this sample owns the same order of the absorptance. We suppose that it may be due to its significant height; therefore, it becomes more effective in light trapping than the others.

IV. CONCLUSIONS

We fabricated black silicon surfaces in a high throughput process based on DRIE at cryogenic temperatures. We studied the influence of various parameters of the etching process on both morphological and optical properties. The reflectance measurements of these structures were performed over a large spectral range from the visible to the mid-infrared. It is found that the average reflectance of the BS samples is clearly correlated to the aspect ratio; it decreases as the aspect ratio of the structure increases. Furthermore, for a given aspect ratio, it is found that the reflectance is inversely proportional to the microstructure height. It is also noted that black silicon surface obtained by this technique

presents a reflectance of about 1% in the visible range. Besides, we reported the absorptance of BS samples in the infrared spectral range (1.3–17 μm). A greatly enhanced absorptance of BS (compared to flat silicon) is observed up to about 75% and it is ascribed to be from the high aspect ratio and the height of the silicon cones, which strongly influence the ability of light trapping. The excellent optical properties of microstructured silicon cones and the simplicity of the fabrication technique provide obtaining high quality black silicon surfaces, with optimized properties thanks to controlled process conditions.

ACKNOWLEDGMENTS

The authors would like to thank Professor Dan Angelescu for his valuable advices throughout this study. We acknowledge also the EADS Foundation for the financial support through the project TESEER.

[1]J. Zhao and M. A. Green, IEEE Trans. Electron Devices **38**, 1925 (1991).
[2]D. Bouhafsa, A. Moussia, A. Chikouchea, and J. M. Ruizb, Sol. Energy Mater. Sol. Cells **52**, 79 (1998).
[3]B. S. Richards, Sol. Energy Mater. Sol. Cells **79**, 369 (2003).
[4]C. Wu, C. H. Crouch, L. Zhao, J. E. Carey, R. Younkin, J. A. Levinson, E. Mazur, R. M. Farrell, P. Gothoskar, and A. Karger, Appl. Phys. Lett. **78**, 1850 (2001).
[5]L. L. Ma, Y. C. Zhou, N. Jiang, X. Lu, J. Shao, W. Lu, J. Ge, X. M. Ding, and X. Y. Hou, Appl. Phys. Lett. **88**, 171907 (2006).
[6]Y. Li, G. J. Feng, and L. Zhao, Adv. Mater. Res. **287–290**, 364 (2011).
[7]J. S. Yoo, I. O. Parm, U. Gangopadhyay, K. Kim, S. K. Dhungel, D. Mangalaraj, and J. Yi, Sol. Energy Mater. Sol. Cells **90**, 3085 (2006).
[8]Y. Xia, B. Liu, J. Liu, Z. Shen, and C. Li, Sol. Energy **85**, 1574 (2011).
[9]D. Murias, C. Reyes-Betanzo, M. Moreno, A. Torres, A. Itzmoyotl, R. Ambrosio, M. Soriano, J. Lucas, and P. Roca i Cabarrocas, Mater. Sci. Eng., B **177**, 1509 (2012).
[10]X. Bao, F. Liu, and X. Zhou, Optik **123**, 1474 (2012).
[11]Z. Huang, J. E. Carey, M. Liu, X. Guo, E. Mazur, and J. C. Campbell, Appl. Phys. Lett. **89**, 033506 (2006).
[12]K. Yamamoto, A. Sakamoto, T. Nagano, and K. Fukumitsu, Nucl. Instrum. Methods Phys. Res. A **624**, 520 (2010).
[13]K. N. Nguyen, D. Abi-Saab, P. Basset, E. Richalot, M. Malak, N. Pavy, F. Flourens, F. Marty, D. Angelescu, Y. Leprince-Wang, and T. Bourouina, Microsyst. Technol. **18**, 1807 (2012).
[14]K. Richter, C. Kubasch, and J.-W. Bartha, Plasma Processes Polym. **4**, S411 (2007).
[15]G. Yuan, R. Mitdank, A. Mogilatenko, and S. F. Fischer, J. Phys. Chem. C **116**, 13767 (2012).
[16]T. Baldacchini, J. E. Carey, M. Zhou, and E. Mazur, Langmuir **22**, 4917 (2006).
[17]N. Gaber, M. Malak, X. C. Yuan, K. N. Nguyen, P. Basset, E. Richalot, D. Angelescu, and T. Bourouina, Lab Chip **13**, 826 (2013).
[18]A. Serpengüzel, A. Kurt, I. Inanç, J. Carey, and E. Mazur, J. Nanophotonics **2**, 21770 (2008).
[19]T. Chen, J. Si, X. Hou, S. Kanehira, K. Miura, and K. Hirao, J. Appl. Phys. **110**, 073106 (2011).
[20]J. I. Gittleman, E. K. Sichel, H. W. Lehmann, and R. Widmer, Appl. Phys. Lett. **35**, 742 (1979).
[21]H. G. Craighead, R. E. Howard, and D. M. Tennant, Appl. Phys. Lett. **37**, 653 (1980).
[22]M. Schnell, R. Ludemann, and S. Schaefer, in *Conference Record of the 28th IEEE Photovoltaic Specialists Conference 2000, Anchorage, Alaska, 15–22 September* (2000), pp. 367–370.
[23]H. Jansen, M. de Boer, and M. Elwenspoek, in *The 9th Annual International Workshop on "An Investigation of Micro Structures, Sensors, Actuators, Machines and Systems," Micro Electro Mechanical Systems, 1996, MEMS '96: Proceedings of IEEE, San Diego, California, USA, 11-15 February* (1996), pp. 250–257.
[24]M. J. De Boer, J. G. E. Gardeniers, H. V. Jansen, E. Smulders, M. J. Gilde, G. Roelofs, J. N. Sasserath, and M. Elwenspoek, J. Microelectromech. Syst. **11**, 385 (2002).
[25]F. Marty, L. Rousseau, B. Saadany, B. Mercier, O. Français, Y. Mita, and T. Bourouina, Microelectron. J. **36**, 673 (2005).
[26]R. Dussart, X. Mellhaoui, T. Tillocher, P. Lefaucheux, M. Volatier, C. Socquet-Clerc, P. Brault, and P. Ranson, J. Phys. D: Appl. Phys. **38**, 3395 (2005).
[27]L. Sainiemi, V. Jokinen, A. Shah, M. Shpak, S. Aura, P. Suvanto, and S. Franssila, Adv. Mater. **23**, 122 (2011).
[28]J. D. Hylton, A. R. Burgers, and W. C. Sinke, J. Electrochem. Soc. **151**, G408 (2004).
[29]M. J. Stocks, A. J. Carr, and A. W. Blakers, Sol. Energy Mater. Sol. Cells **40**, 33 (1996).
[30]S. K. Srivastava, D. Kumar, Vandana, M. Sharma, R. Kumar, and P. K. Singh, Sol. Energy Mater. Sol. Cells **100**, 33 (2012).
[31]R. Younkin, J. E. Carey, E. Mazur, J. A. Levinson, and C. M. Friend, J. Appl. Phys. **93**, 2626 (2003).
[32]C. H. Crouch, J. E. Carey, M. Shen, E. Mazur, and F. Y. Génin, Appl. Phys. A **79**, 1635 (2004).
[33]M.-J. Sher, M. T. Winkler, and E. Mazur, MRS Bull. **36**, 439 (2011).
[34]R. Dussart, M. Boufnichel, G. Marcos, P. Lefaucheux, A. Basillais, R. Benoit, T. Tillocher, X. Mellhaoui, H. Estrade-Szwarckopf, and P. Ranson, J. Micromech. Microeng. **14**, 190 (2004).
[35]X. Mellhaoui, R. Dussart, T. Tillocher, P. Lefaucheux, P. Ranson, M. Boufnichel, and L. J. Overzet, J. Appl. Phys. **98**, 104901 (2005).
[36]E. D. Diebold, N. H. Mack, S. K. Doom, and E. Mazur, Langmuir **25**, 1790 (2009).
[37]See supplementary material at http://dx.doi.org/10.1063/1.4805024 for modelling of black silicon and numerical simulations.
[38]S. Kalem, P. Werner, Ö. Arthursson, V. Talalaev, B. Nilsson, M. Hagberg, H. Frederiksen, and U. Södervall, Nanotechnology **22**, 235307 (2011).
[39]Y. Kato and S. Adachi, Appl. Surf. Sci. **258**, 5689 (2012).